Electronic Supplementary Material (ESI) for Nanoscale.

Hierarchically Structured Silver-Iron Lotus Flowers for Efficient Oxygen Reduction Reaction (ORR)

Gumaa A. El-Nagar*[a,b], Iver Lauermann [c], Radwan M. Sarhan[a], and Christina Roth*[b]

Supplementary information

Experimental Section

Chemicals

All the used chemicals in this study are analytical grade used without any further refinement. $AgNO_3$ (ultra-pure, 99.99%), L-ascorbic acid (99%), Iron (III) nitrate nonahydrate (≥99.95%), and succinic acid (ACS reagent, ≥99%) are purchased from Sigma-Aldrich. Deionized water with resistivity of 18.2 MΩ cm prepared by a Milli-Q reagent deionizer (Millipore) was used to prepare all solutions.

Material Characterization

The morphology and bulk composition of the as-prepared silver structures were evaluated by scanning electron microscopy (SEM, HITACHI UHR FE-SEM SU8030) coupled with an energy dispersive X-ray spectrometer (EDS). The materials' crystal structure was investigated by X-ray diffraction (XRD) in transmission geometry using a STOE STADI operated with Cu Kα (λ = 1.54 Å) radiation and position sensitive detector. Furthermore, X-ray photoelectron spectroscopy (XPS, CLAM4 electron analyzer from Thermo VG scientific), using a Mg Kα X-ray source (1254 eV) was used to determine the samples chemical composition.

Electrochemical Measurements

Electrochemical measurements were carried out with a Galvanostat/Potentiostat Reference 3000 (Gamry Instruments) at room temperature in a conventional three-electrode glass cell with a Pt spiral as a counter electrode, saturated calomel electrode (SCE with potential of 0.238 V) as a reference electrode and glassy carbon electrode loaded with different catalysts as a working electrode. 28 μg/cm^2 of the as-prepared catalysts ink were supported atop a glassy carbon electrode surface or a glassy carbon rotating disk electrode surface (3 mm in diameter). The scan rate was 5 mV/s for all electrochemical measurements. The performance of the as-prepared silver-based structures was investigated in O_2-saturated 0.1 M KOH aqueous solution using a rotating disk electrode (RDE) setup. Electrochemical impedance spectroscopy (EIS) measurements were performed at – 10 mV vs. SCE with a disturbance potential of 5 mV and a frequency range from 1 MHz to 0.1 Hz. Current transients (I-t) measured at -100 mV vs. SCE in O2-saturated 0.1 M KOH.

Electrode Preparation

The working electrode was prepared as follows: first, Ag and Ag-Fe catalysts were dispersed on carbon Vulcan XC-72R with 40% Ag and Ag-Fe. Then, 3 mg of the as-prepared catalyst was dispersed in 750 μl deionized water and 250 μl isopropanol solution containing 20 μl of Nafion aqueous solution. The above mixture was then ultra-sonicated for 2 h to obtain a homogeneous catalyst ink. In order to prepare the working electrode for the electrochemical measurements, certain volumes of the freshly prepared ink was cast onto the mirror polished glassy carbon electrode followed by drying in air.

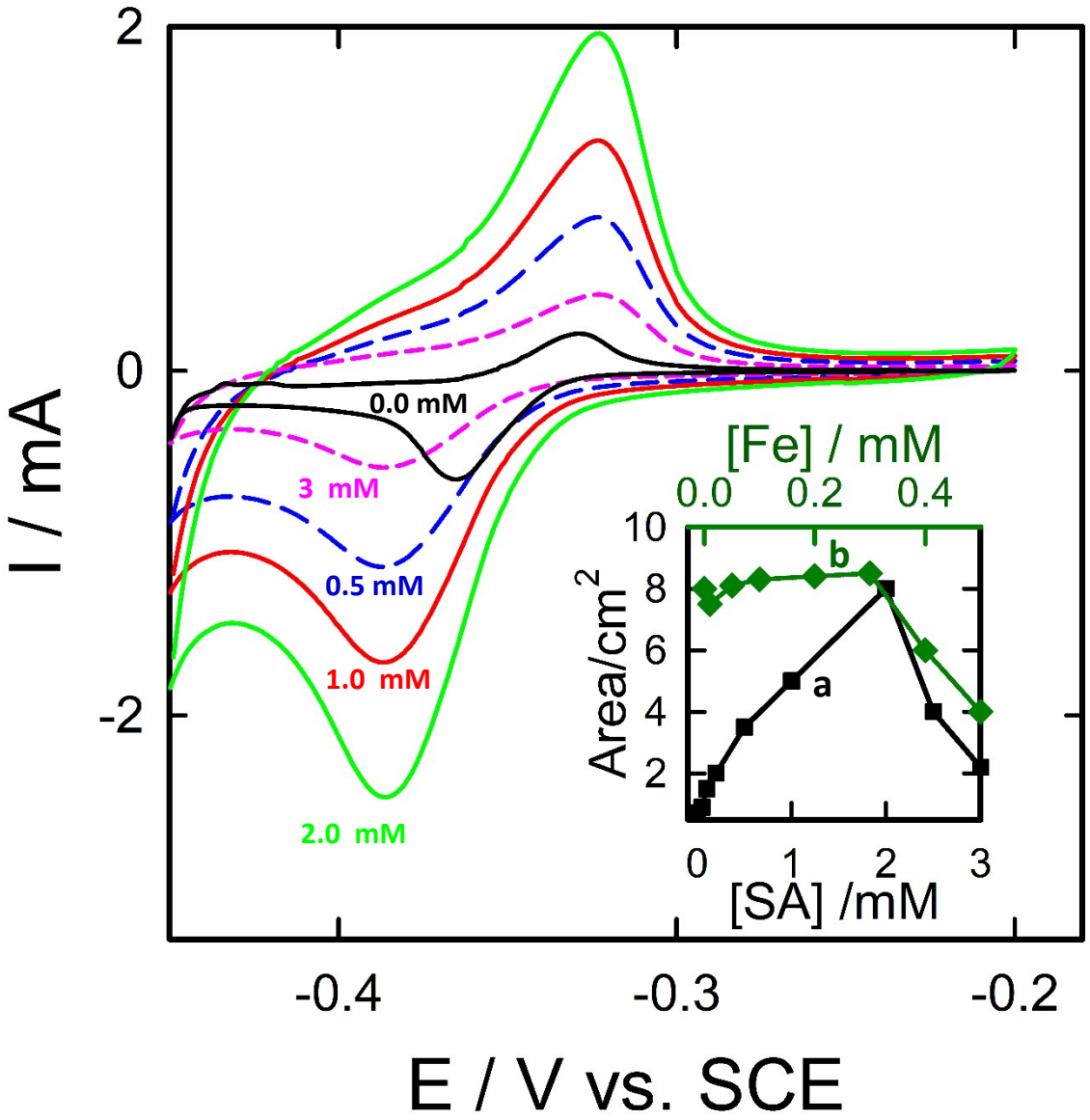

Figure S1: Pb (UPD) stripping measured in 0.1 M HCl containing 10 mM $Pb(NO_3)_2$ obtained at Ag flowers created using various SA concentrations. This experiment was used to estimate the electrochemically active surface area of the as-prepared Ag-Fe structures as described in our recent publication[1]. Inset shows the variation of the electrochemically active surface area of (a) Ag particles with SA concentration and (b) Ag-Fe created using 2 mM SA with iron concentrations (green line and green X-axis). As clearly seen in this figure, the electrochemically active surface area of Ag particles increased with the increase of the SA concentration, reached a maximum at 2 mM SA and then decreased. This reduction of the area is attributed to the deterioration of the flower-structures at higher SA concentrations, as indicated from Figure 1 E&F. Additionally, the insertion of iron particles in the optimized Ag particles prepared using 2 mM SA does not change the area so much compared to Ag structures created using 2 mM as long as iron concentrations lower than 0.2 mM were applied. Further increase of the iron concentration resulted in a significant decrease of the active area, attributed to the destruction of the flower-like structures as indicated from Figure 1 K&L Ag-Fe.

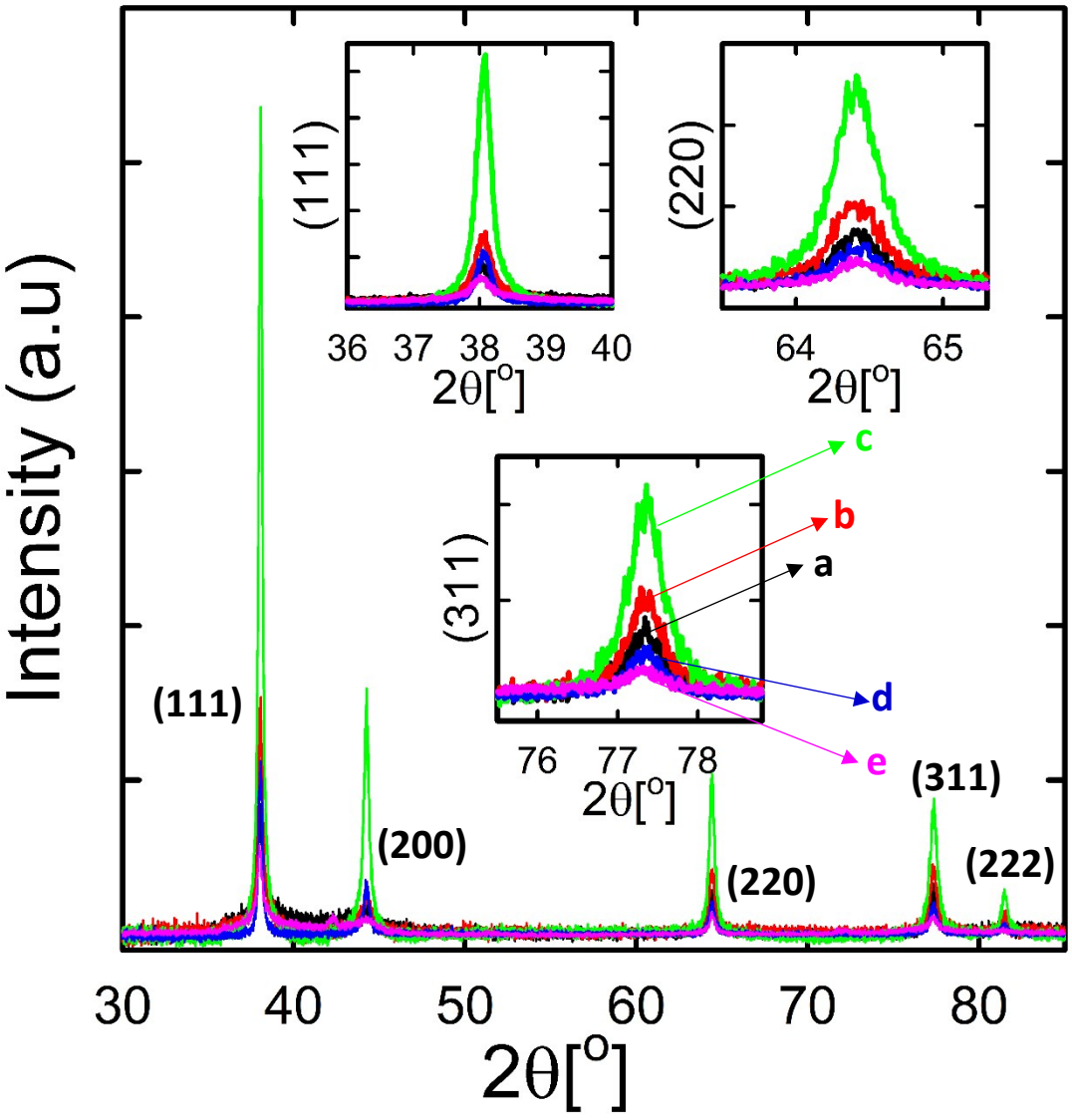

Figure S2A: XRD patterns of Ag structures prepared using different SA concentrations, typically, (a) 0.0 mM, (b) 0.5 mM, (c) 2 mM, (d) 2.5 mM and (e) 3 mM SA.

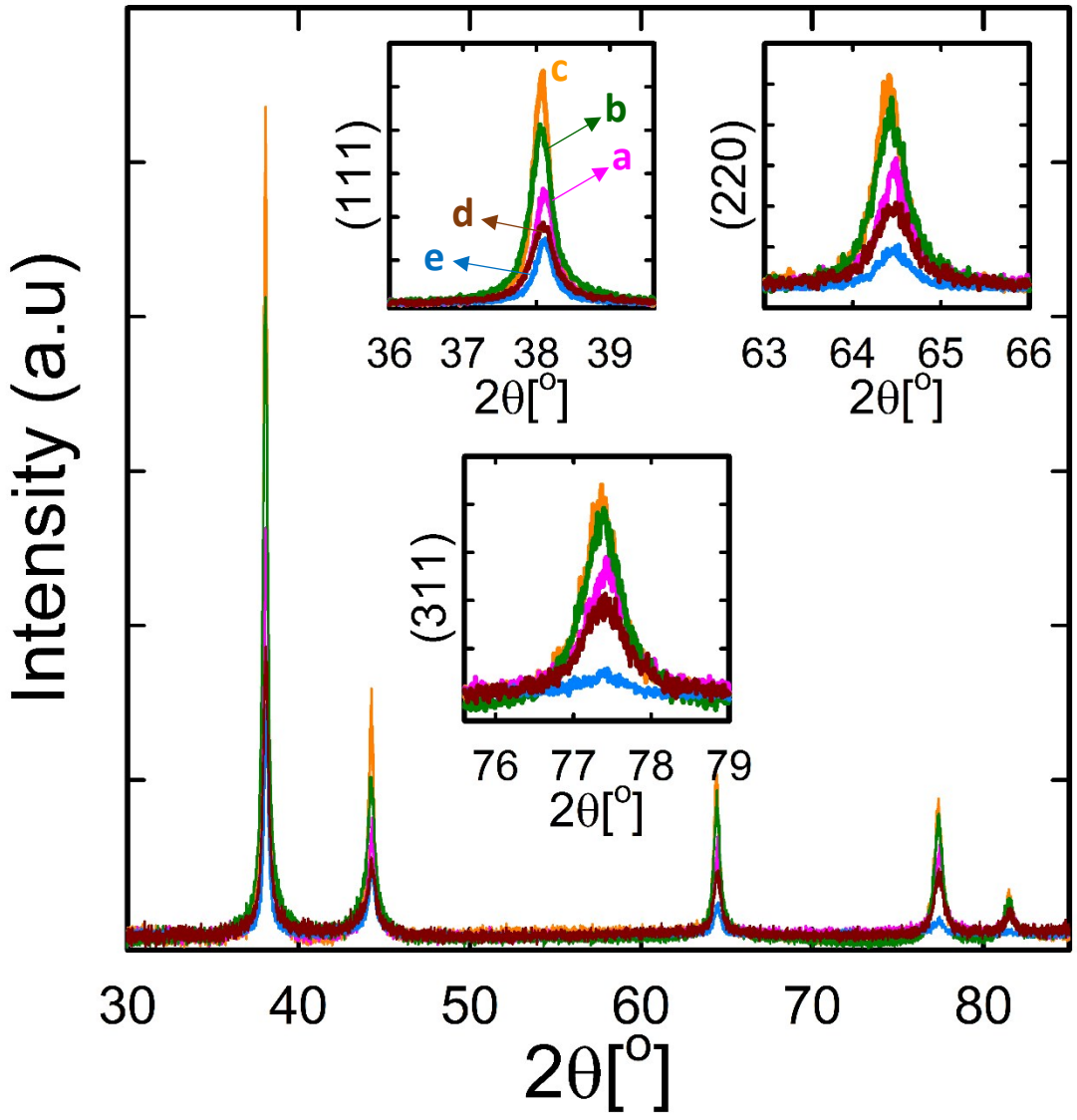

Figure S2B: XRD patterns of Ag-Fe structures prepared using 2 mM SA and different Fe concentrations, typically, (a) 0.0 mM, (b) 0.1 mM, (c) 0.2 mM, (d) 0.3 mM and (e) 0.4 mM iron.

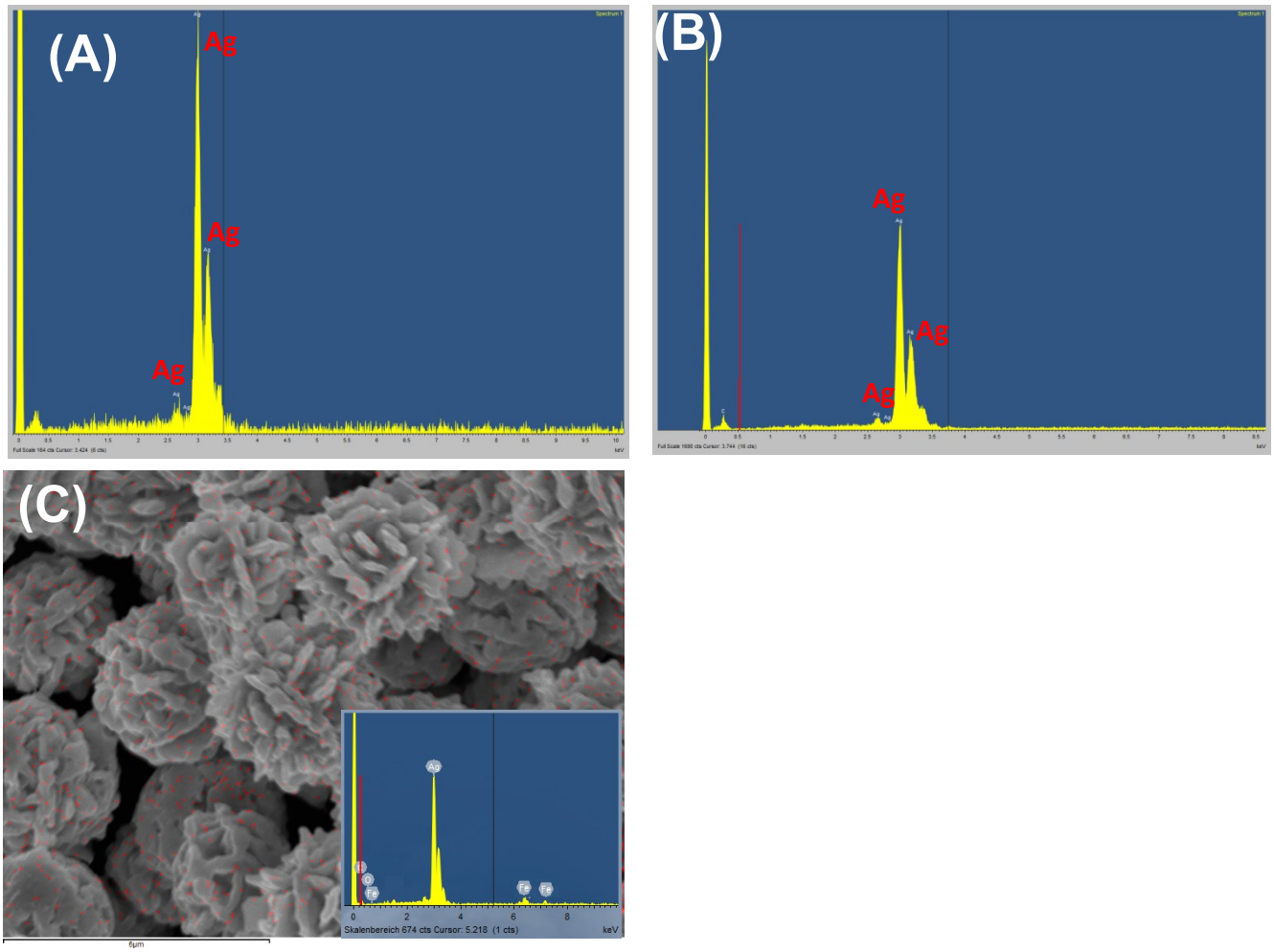

Figure S3: EDX analysis of (A) Ag_{ball} (obtained without using SA), (B) $Ag_{chrysan.}$ (Prepared using 2mM SA) and (C) EDX analysis and respective Fe mapping of the Ag-Fe structure(created using 2 mM SA and 0.1 mM iron). As seen in this figure, EDS analysis of Ag_{ball} and $Ag_{chrysan}$ shows only three strong peaks for silver and a small peak for carbon (carbon might be attributed to the surfactant or the used carbon tape). While the Ag-Fe spectrum exhibits two additional peaks for iron, besides the silver and carbon peaks. Mapping analysis of Ag-Fe shows the homogenous distribution of iron on silver flowers.

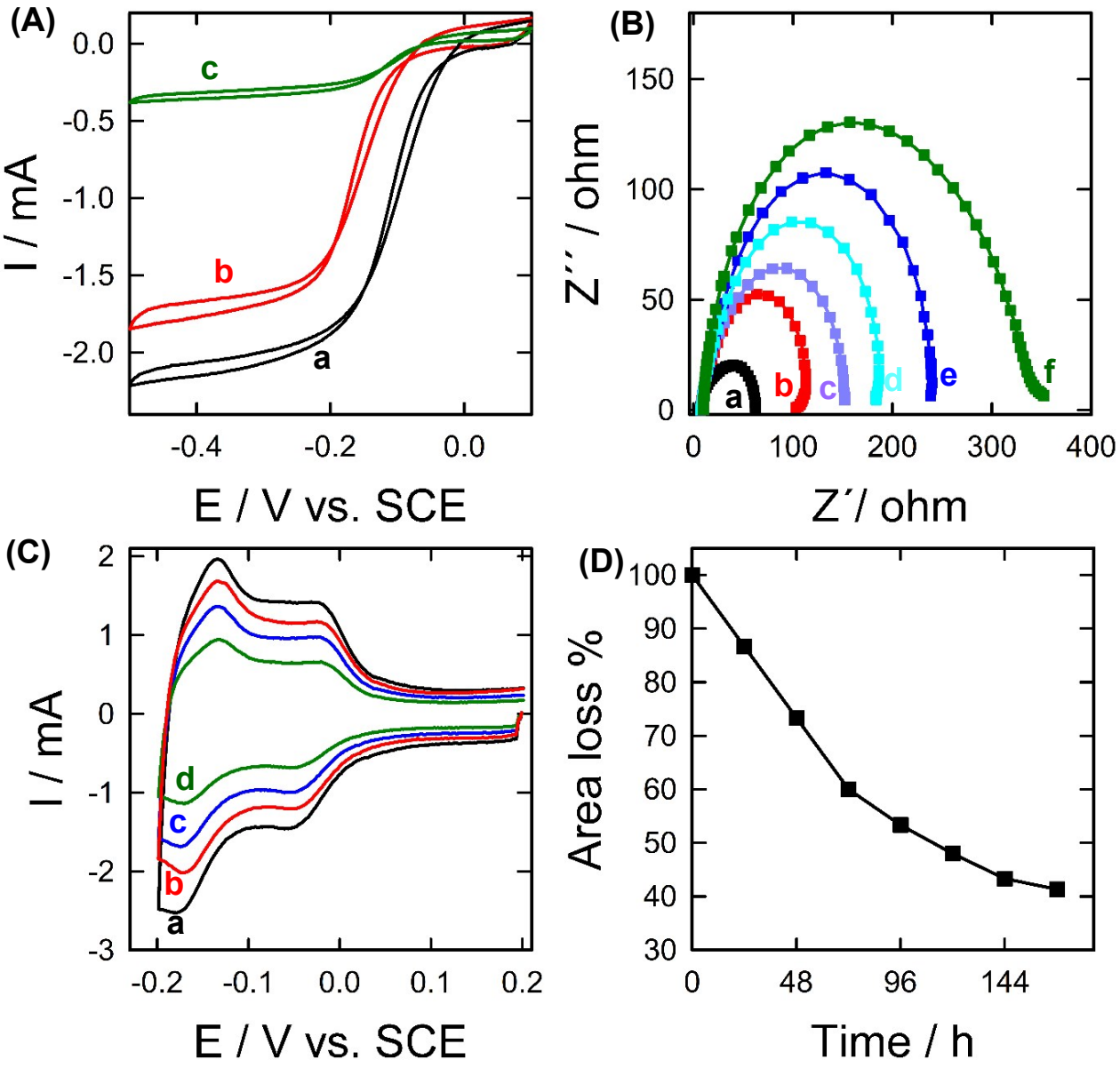

Figure S4: (A) LSVs obtained at PtC in O_2-saturated 0.1 M KOH solution before (a) and after (b&c) measuring current transients (i-t plot) at -0.15 V vs SCE for (b) 2 days and (c) 7 days. (B) Nyquist plots obtained at PtC in O_2-saturated 0.1 M KOH solution before (a) and after (b) 1 day, (c) 2 days, (d) 3 days, (e) 5 days and (f) 7 days of continuous electrolysis at -0.15 V vs. SCE. (C) CVs of PtC in 0.1 M N2-saturated $HClO_4$ solution before (a) and after 1, 3 and 7 days of continuous ORR electrolysis curves b, c and d, respectively. (D) Variation of the electrochemically active surface area loss of PtC electrode as calculated from Figure S4 C with time of continuous ORR electrolysis.

As seen in this figure, the ORR electrocatalytic activity of the commercial PtC electrode significantly decreased with time (Figure S4A). This performance deterioration is attributed to the significant increase of the ORR charge transfer resistance (Figure S4B) along with a large reduction of the Pt electrochemically active surface area (Figure S4C&D).

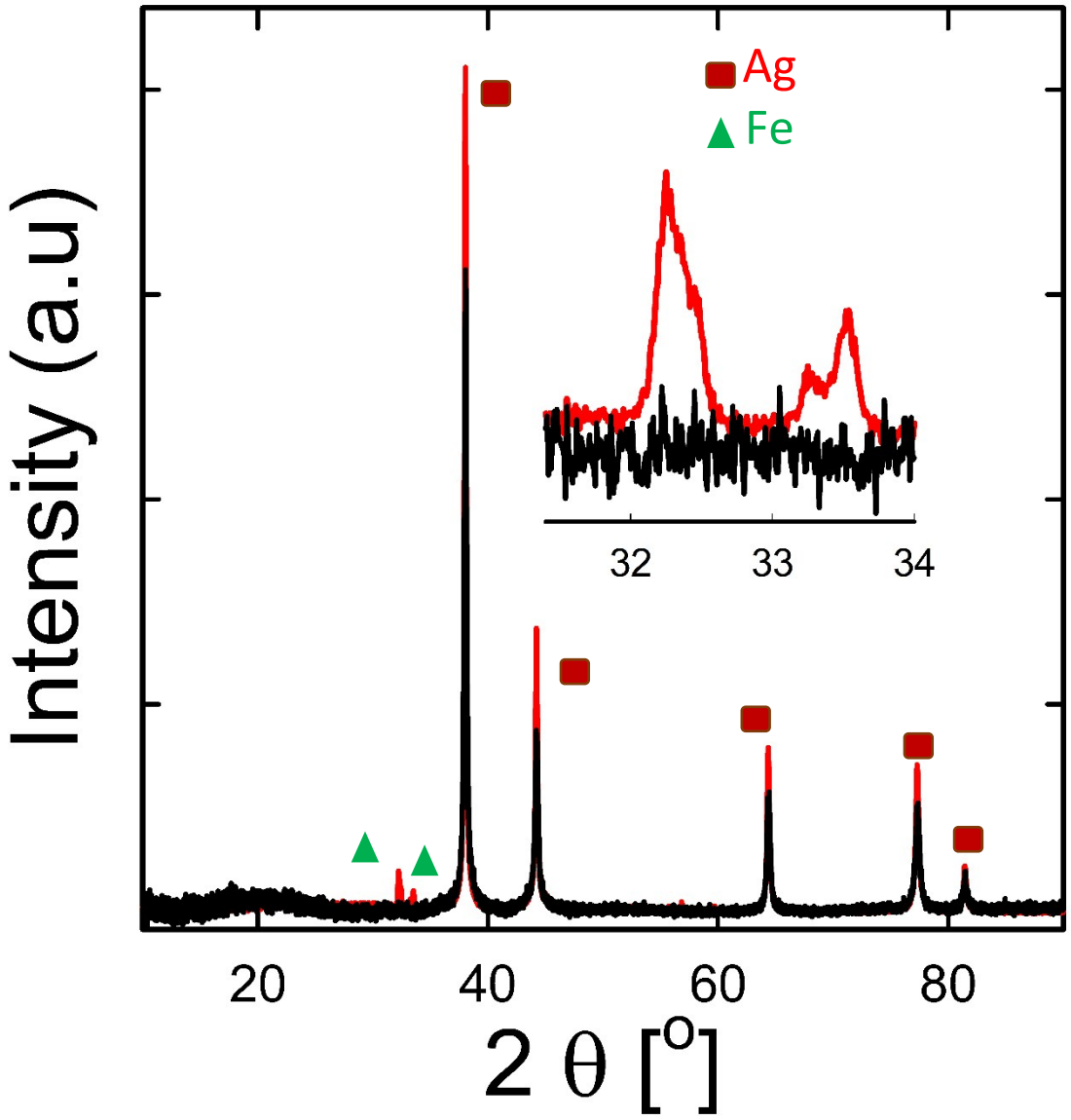

Figure S5: XRD patterns of $AgFe_{lotus}$ before (black-plot) and after (read-plot) ORR electrolysis. After measurements two new diffraction peaks are observed as shown in inset of Figure S6 which can be assigned to Iron.

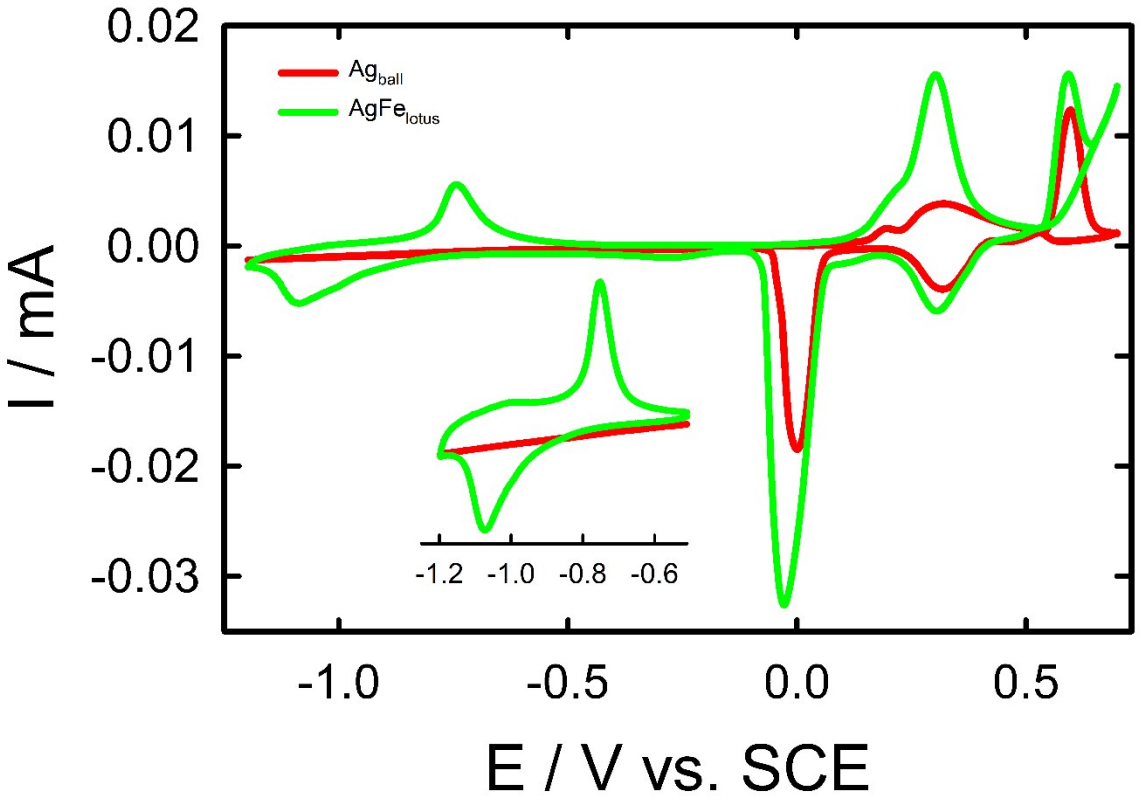

Figure S6: CVs of Ag_{ball} and $AgFe_{lotus}$ with 10% iron weight percent in 0.1 M KOH with scan potential of 50 mV/s. Inset shows the Fe^{2+}/Fe^{3+} transformation

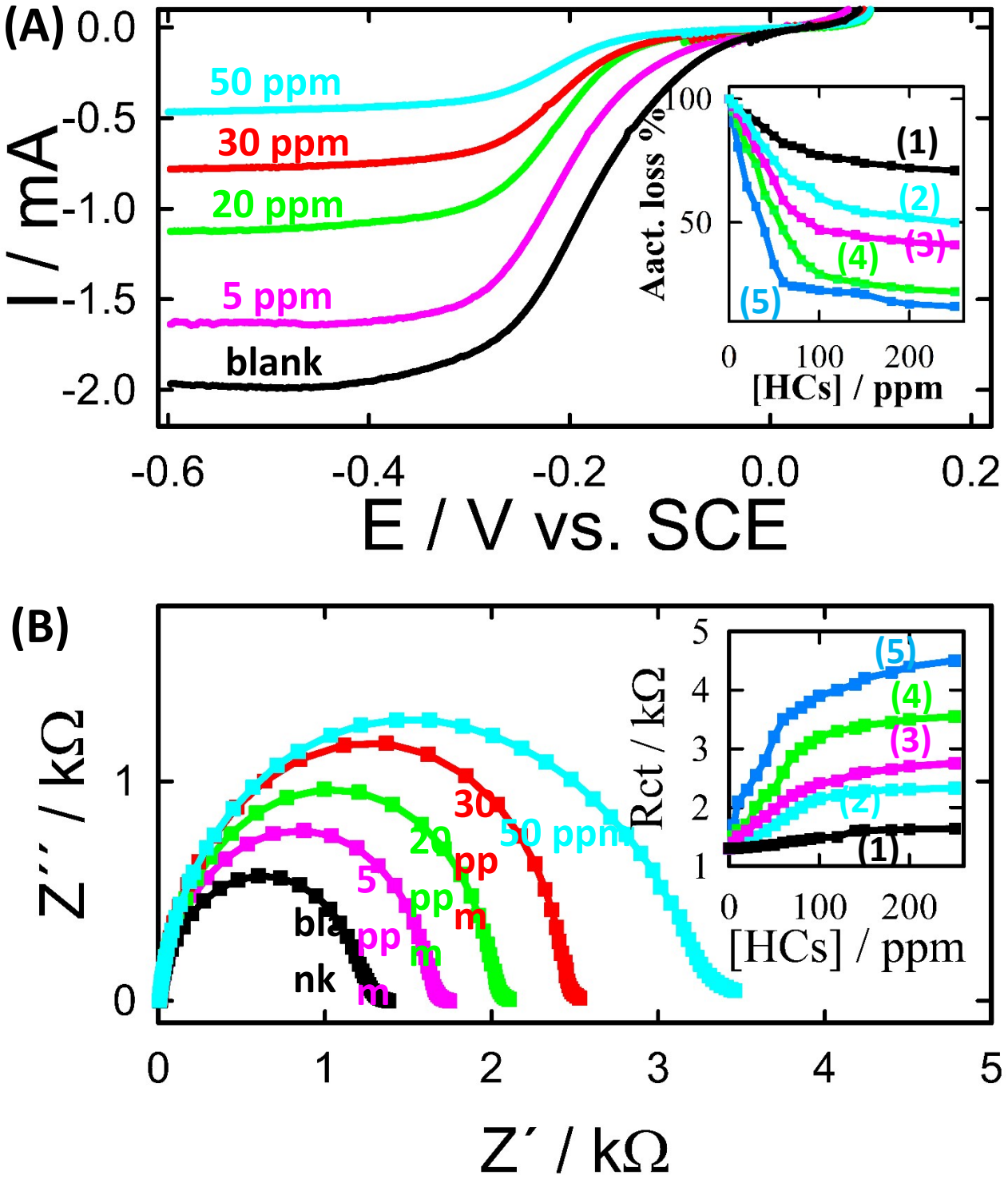

Figure S7. (A) LSVs obtained at PtC in the presence of various acetonitrile concentrations. Insets show the variation of their respective activity with concentration of different HCs impurities (typically, acetonitrile (5), acrylonitrile (4), triethyl amine (3), vinyl acetate (2) and toluene (1)). (B) Their respective Nyquist plots in O_2-saturated 0.1 M KOH containing various acetonitrile concentrations. Insets show the variation of their respective charge transfer resistance in presence of various HCs impurities concentrations. Note that the same electrodes, colors and notations are used as in Figure S6A.

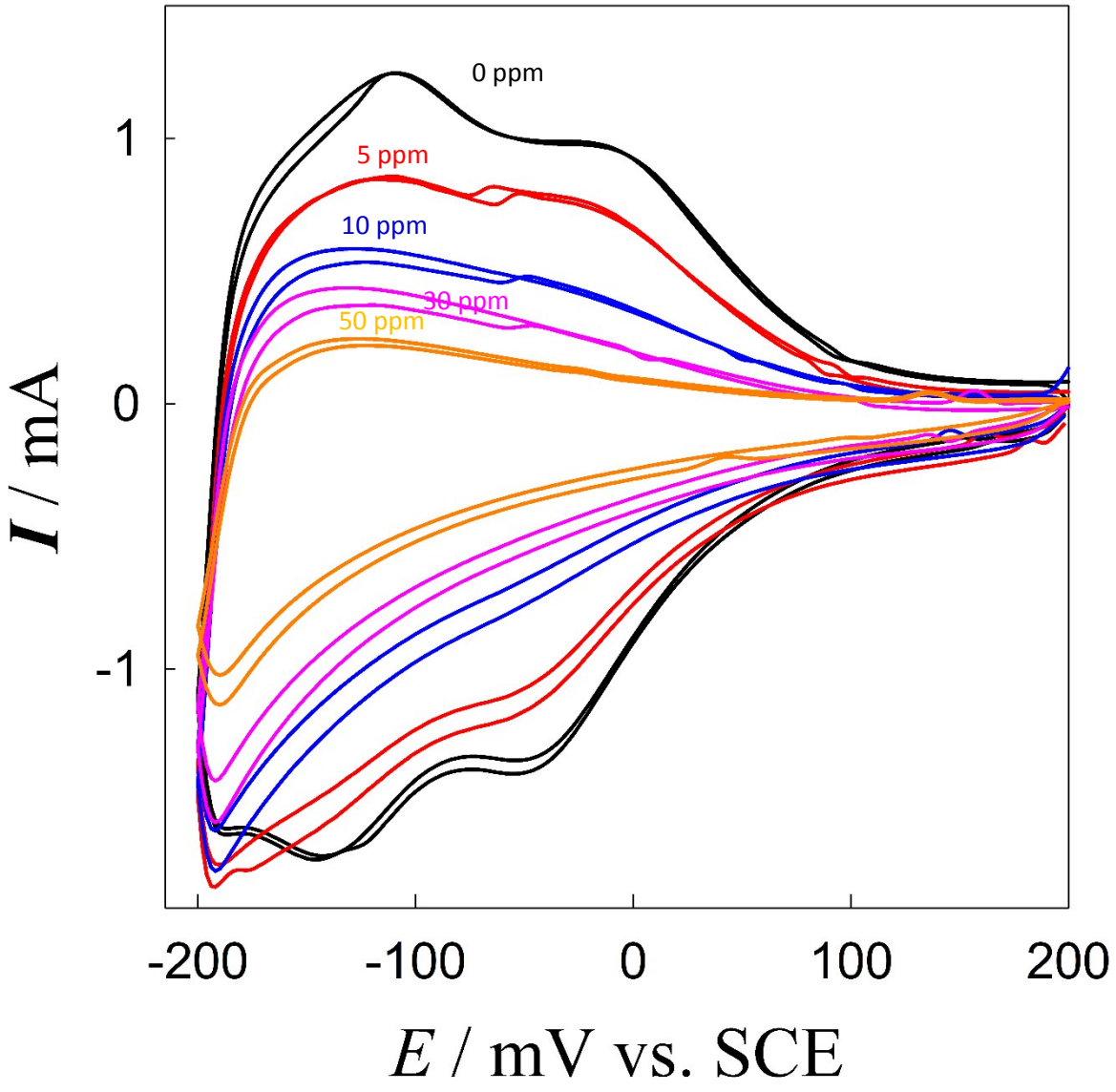

Figure S8: CVs obtained at PtC in N_2-saturated 0.1 M $HClO_4$ solution in the absence (a) and presence of various acetonitrile concentrations (b-e), typically 1 ppm, 10 ppm, 50 ppm and 100 ppm acetonitrile.

Table S1: lists and compares the estimated average particle sizes and the (111)/(220) diffraction peaks ratio of the undoped and iron-doped silver particles created using different capping agent concentrations.

Silver Particles			*Iron-doped Silver Particles*		
SA Conc./ mM	*Particle Size/nm*	*(111)/(220)*	*Fe Conc. / mM*	*Particle Size/nm*	*(111)/(220)*
0.0	*102*	*3.2*	*0.04*	*62*	*5.1*
0.4	*91*	*4.4*	*0.10*	*67*	*5.4*
1.0	*69*	*5.2*	*0.20*	*64*	*5.6*
2.0	*58*	*5.8*	*0.30*	*59*	*5.7*
2.4	*64*	*4.17*	*0.40*	*63*	*4.8*
3.0	*87*	*4.11*	*0.60*	*75*	*4.0*

Table S2: comparison between our suggested ORR catalysts with recently reported ORR electrocatalysts.

Electrocatalyst	E1/2 (V vs. RHE)	Max. current mA cm^{-2}	Tafel slopes mV dec^{-1}	Onset Potential (V vs. RHE)	References
AgFePC	0.931	-6	34	0.99	[2]
Co3O4/N-CP-900	0.90	-5.5	-	0.97	[3]
BG-AgNWs	0.84	-5.88	90	~0.87*	[4]
AgCo alloy	~0.83*	-4.0	-	~0.87*	[5]
Ag/N-RGO	0.76	-5.3	70	0.96	[6]
AgCu core-shell	0.79	-5.8	-	-	[7]
Ag/Co-NGr	0.82	-4.6	73	0.90	[8]
$AgFe_{lotus}$	0.93	-5.3	47	0.99	This work
Commercial PtC	0.89	-5.1	95	0.98	This work

References

[1] El-Nagar GA, Sarhan RM, Abouserie A, Maticiuc N, Bargheer M, Lauermann I, et al. Efficient 3D-Silver Flower-like Microstructures for Non-Enzymatic Hydrogen Peroxide (H2O2) Amperometric Detection. Scientific Reports. 2017;7:12181.
[2] Miller HA, Bevilacqua M, Filippi J, Lavacchi A, Marchionni A, Marelli M, et al. Nanostructured Fe-Ag electrocatalysts for the oxygen reduction reaction in alkaline media. Journal of Materials Chemistry A. 2013;1:13337-47.
[3] Lin Z, Qiao X. Coral-like Co3O4 Decorated N-doped Carbon Particles as active Materials for Oxygen Reduction Reaction and Supercapacitor. Scientific Reports. 2018;8:1802.
[4] Nair AK, Thazhe veettil V, Kalarikkal N, Thomas S, Kala MS, Sahajwalla V, et al. Boron doped graphene wrapped silver nanowires as an efficient electrocatalyst for molecular oxygen reduction. Scientific Reports. 2016;6:37731.
[5] Holewinski A, Idrobo J-C, Linic S. High-performance Ag–Co alloy catalysts for electrochemical oxygen reduction. Nature Chemistry. 2014;6:828.
[6] Li S, Miao H, Xu Q, Xue Y, Sun S, Wang Q, et al. Silver nanoparticles supported on a nitrogen-doped graphene aerogel composite catalyst for an oxygen reduction reaction in aluminum air batteries. RSC Advances. 2016;6:99179-83.
[7] Zhang N, Chen F, Wu X, Wang Q, Qaseem A, Xia Z. The activity origin of core-shell and alloy AgCu bimetallic nanoparticles for the oxygen reduction reaction. Journal of Materials Chemistry A. 2017;5:7043-54.
[8] Qaseem A, Chen F, Wu X, Zhang N, Xia Z. Ag, Co/graphene interactions and its effect on electrocatalytic oxygen reduction in alkaline media. Journal of Power Sources. 2017;370:1-13.